CHEMISTRY
A EUROPEAN JOURNAL

DOI: 10.1002/chem.200701923

Exploring Helical Folding of Oligoureas During Chain Elongation by High-Resolution Magic-Angle-Spinning (HRMAS) NMR Spectroscopy

Aude Violette,[a] Nathalie Lancelot,[b] Alexander Poschalko,[a, d] Martial Piotto,[c] Jean-Paul Briand,[a] Jesus Raya,[b] Karim Elbayed,[b] Alberto Bianco,[a] and Gilles Guichard*[a]

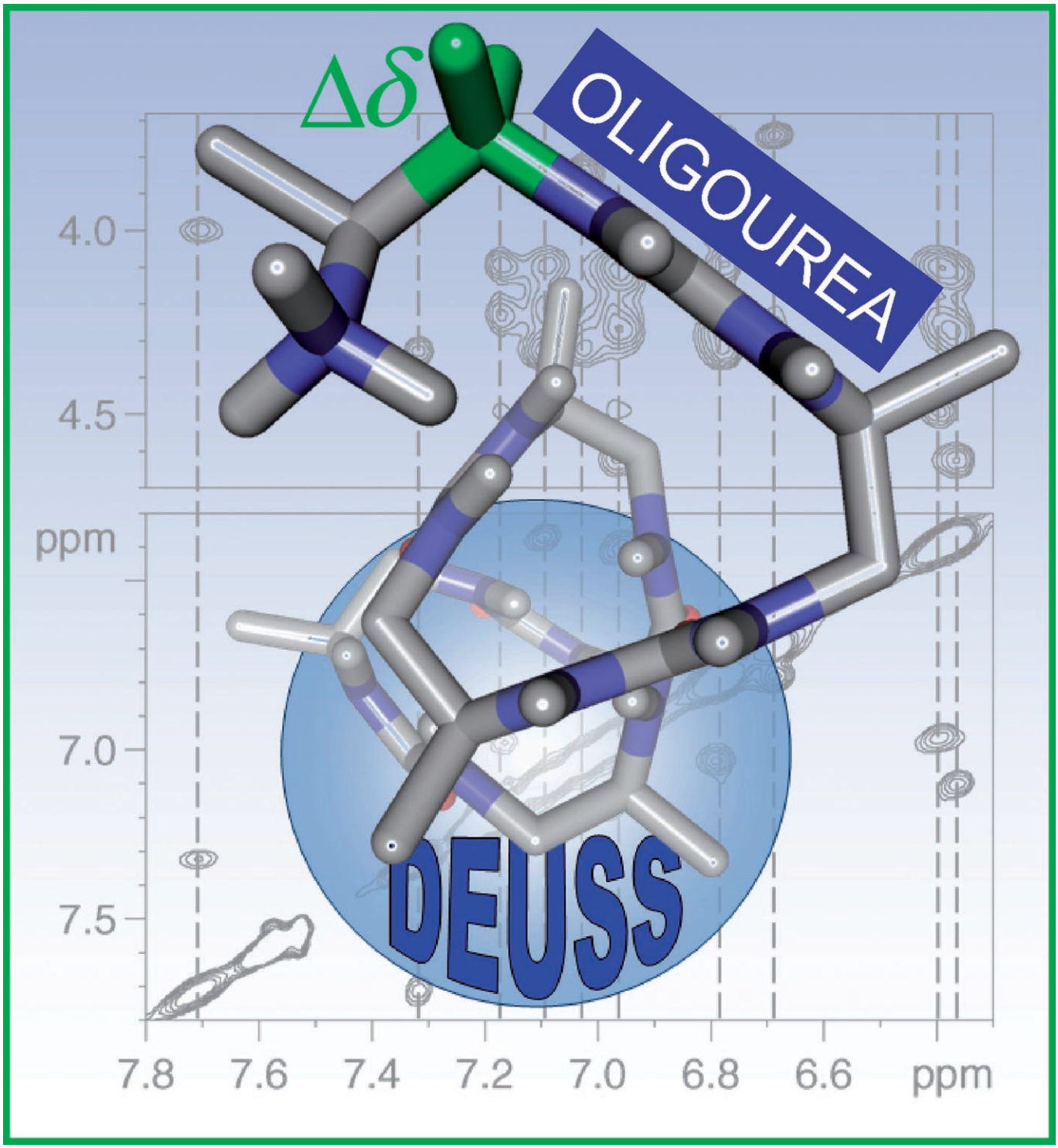

Abstract: The development of novel folding oligomers (foldamers) for biological and biomedical applications requires both precise structural information and appropriate methods to detect folding propensity. However, the synthesis and the systematic conformational investigation of large arrays of oligomers to determine the influence of factors, such as chain length, side chains, and surrounding environment, on secondary structure can be quite tedious. Herein, we show for 2.5-helical *N*,*N*′-linked oligoureas (γ-peptide lineage) that the whole process of foldamer characterization can be accelerated by using high-resolution magic-angle-spinning (HRMAS) NMR spectroscopy. This was achieved by monitoring a simple descriptor of conformational homogeneity (e.g., chemical shift difference between diastereotopic main chain CH_2 protons) at different stages of oligourea chain growth on a solid support. HRMAS NMR experiments were conducted on two sets of oligoureas, ranging from dimer to hexamer, immobilized on DEUSS, a perdeuterated poly(oxyethylene)-based solid support swollen in solvents of low to high polarity. One evident advantage of the method is that only minute amount of material is required. In addition, the resonance of the deuterated resin is almost negligeable. On-bead NOESY spectra of high quality and with resolution comparable to that of liquid samples were obtained for longer oligomers, thus allowing detailed structural characterization.

Keywords: conformation analysis · foldamers · helical structures · NMR spectroscopy · oligoureas

Introduction

Biotic and abiotic oligoamide foldamers have attracted considerable attention in recent years.[1–4] We and others have shown that the urea moiety, by its capacity to form autocomplementary hydrogen bonds can be substituted for the amide linkage to generate open-chain oligomers that self-organize at the molecular level through either local conformational preferences or remote intrastrand interactions to form new structural patterns.[5–7] Enantiopure *N*,*N*′-linked oligoureas with proteinogenic side chains of general formula H-[NH-$^{\beta}$CH(R)-$^{\alpha}$$CH_2$-N′H-CO-]$_n$-$NH_2$ are peptide backbone mimetics belonging to the γ-peptide lineage. In solution, they adopt a well-defined 2.5-helical fold, reminiscent of the γ^4-peptide 14-helix. The structure is stabilized by hydrogen bonds closing both 12- and 14-membered rings and is characterized by a stable (+)-synclinal arrangement around the ethane bonds. The predictability of 2.5-helix formation suggested us that the oligourea backbone could be used as a template to elaborate functional mimetics of bioactive helical α-polypeptides. In particular, short-chain oligoureas designed to mimic globally amphiphilic α-helical host–defense peptides were found to be effective against both gram-negative and gram-positive bacteria.[8] However, both the precise understanding of the factors that govern helix formation and the control of the structure are necessary if these molecules are to be envisaged as tools in biology. With the aim to speed-up the characterization of oligourea foldamers, we have now explored the possibility to directly monitor helix formation of oligoureas bound to a solid support at different stages of chain growth by using high-resolution magic-angle-spinning (HRMAS) NMR spectroscopy. HRMAS NMR spectroscopy is a powerful technique to investigate the structure and mobility of immobilized species including natural oligomers, such as α-peptides.[9–15] Herein, we present the synthesis and HRMAS NMR conformational analysis of two series of *N*,*N*′-linked oligoureas covalently bound to DEUSS,[16] a perdeuterated poly(oxyethylene)-based solid support. Advantages shared by DEUSS and its corresponding nondeuterated version POEPOP[17] include: 1) high swelling capacity in organic solvents and aqueous environment, 2) high quality on-bead NMR spectra, and 3) a resolution close to that of liquid samples. DEUSS resin was introduced by us to facilitate detailed HRMAS NMR studies, the signal intensity of the oxyethylene protons in DEUSS being reduced by two orders of magnitude (i.e. to the level of attached molecules) in comparison to POEPOP.[16]

[a] Dr. A. Violette,[+] Dr. A. Poschalko, Dr. J.-P. Briand, Dr. A. Bianco, Dr. G. Guichard
CNRS, Institut de Biologie Moléculaire et Cellulaire
Immunologie et Chimie Thérapeutiques, 15 rue Descartes
67084 Strasbourg (France)
Fax: (+33) 388-610-680
E-mail: g.guichard@ibmc.u-strasbg.fr

[b] Dr. N. Lancelot,[+] Dr. J. Raya, Dr. K. Elbayed
Universite Louis Pasteur/CNRS LC3-UMR7177
Institut/Faculté de Chimie, 4 rue Blaise Pascal
67070 Strasbourg (France)

[c] Dr. M. Piotto
Bruker Biospin, 34 rue de l'Industrie
67166 Wissembourg (France)

[d] Dr. A. Poschalko
current address: DSM Nutritional Products
R&D Personal Care, Bld. 205/307a, 4070 Basel (Switzerland)

[+] A.V. and N.L. contributed equally to this work.

Supporting information for this article is available on the WWW under http://www.chemeurj.org/ or from the author.

Results and Discussion

Design and preparation of DEUSS-immobilized oligoureas: Two series of immobilized model oligoureas ranging from dimer (**1.1**, **2.1**) to hexamer (**1.5**, **2.5**) have been prepared by stepwise assembly on the amino functionalized DEUSS resin **4** (Figure 1). Compounds in the first series (**1.1**–**1.5**)

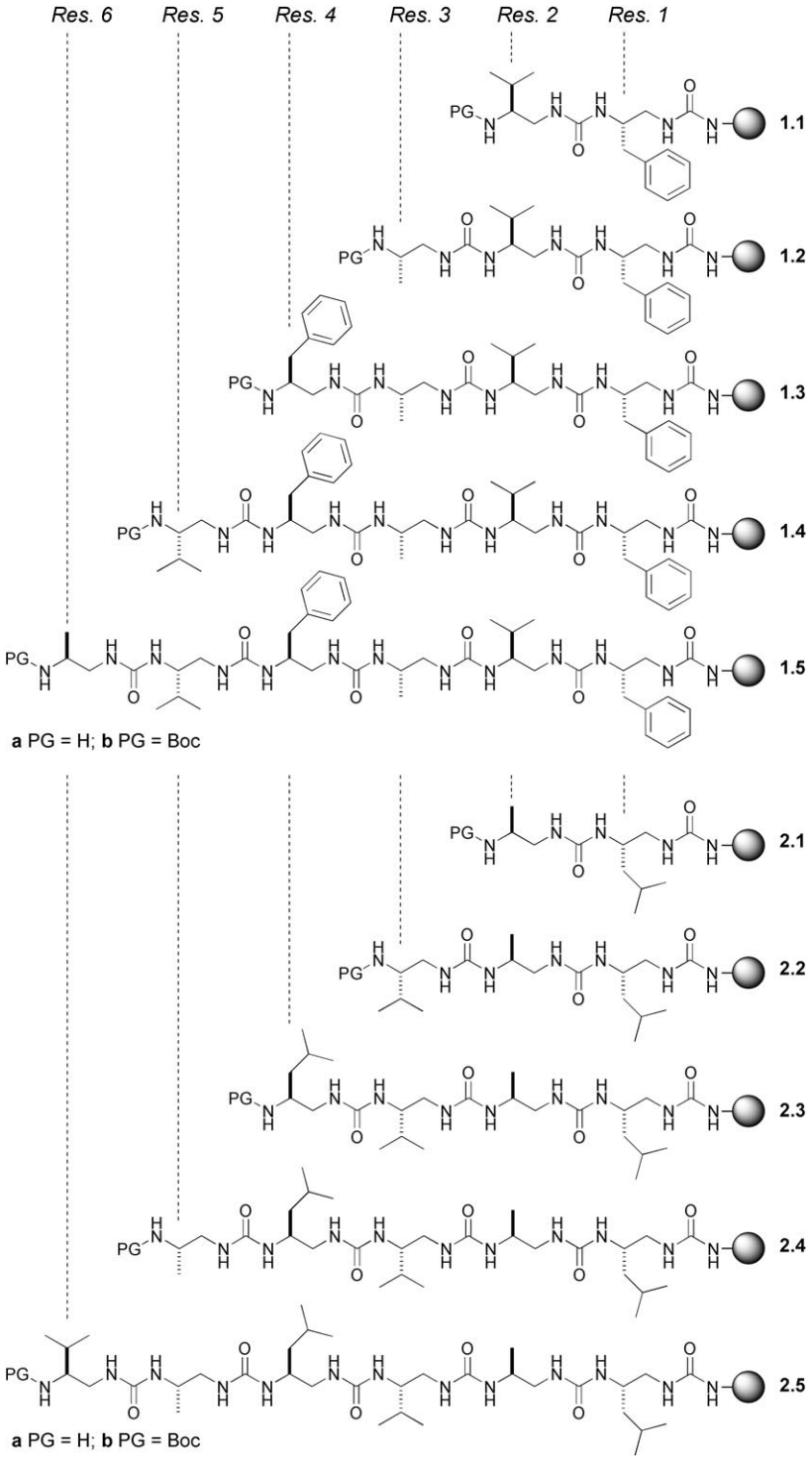

Figure 1. The two series of DEUSS-bound oligoureas prepared for HRMAS NMR analysis. The residue numbering scheme used throughout the paper is indicated.

with alternating side chains of Ala, Val, and Phe were synthesized for comparison with oligoureas previously studied in solution.[5a,c] To investigate possible sequence effects on folding, oligoureas in the second series were exclusively composed of aliphatic side chains.

The syntheses were performed on a 2.5 μmol scale by using succinimidyl {2-{[(*tert*-butoxy)carbonyl]amino}-2-X-ethyl}carbamates or succinimidyl {2-{[(9*H*-fluoren-9-ylmethoxy)-carbonyl]amino}-2-X-ethyl} carbamates as previously described (Scheme 1).[18,19] At the end of the synthesis, the resins were washed with CH_2Cl_2 and diethyl ether, and dried under high vacuum before swelling in the appropriate deuterated solvent for HRMAS NMR analysis. Because the oligourea–DEUSS resins were analyzed directly at the end of the synthesis without the possibility to further purify the oligomers, it was mandatory to keep coupling and deprotection yields extremely high during the whole synthesis. Whereas the use of *N*-Fmoc-protected (Fmoc = 9-fluorenylmethoxycarbonyl) building blocks proved unsatisfactory with the presence of many impurities detected by HRMAS NMR analysis, the Boc (Boc = *tert*-butoxycarbonyl) strategy gave very good results with no significant impurities visible in the HRMAS NMR spectra recorded.[20]

Chain length dependence and capping effect: Resin-bound oligoureas **1.1** to **1.5** and **2.1** to **2.5** bearing either a free or a Boc-protected amino terminal end were swollen in $[D_3]$MeCN and analyzed by HRMAS NMR spectroscopy at 300 K using a combination of DIPSI2 ($\tau_m = 60$ ms), ^{1}H-^{13}C HSQC and NOESY ($\tau_m = 300$ ms) experiments. Samples were spun at 6–7 kHz. Qualitative comparison of spectra was very informative. The quality and the dispersion of the signals were found to depend on both the sequence and the length of oligoureas studied. Whereas resonances of diurea **1.1** were readily assigned (portions of DIPSI2 and ^{1}H-^{13}C HSQC spectra of **1.1b** are shown in Figure 2a), complete spin-system assignment of intermediate triurea **1.2**, tetraurea **1.3**, and pentaur-

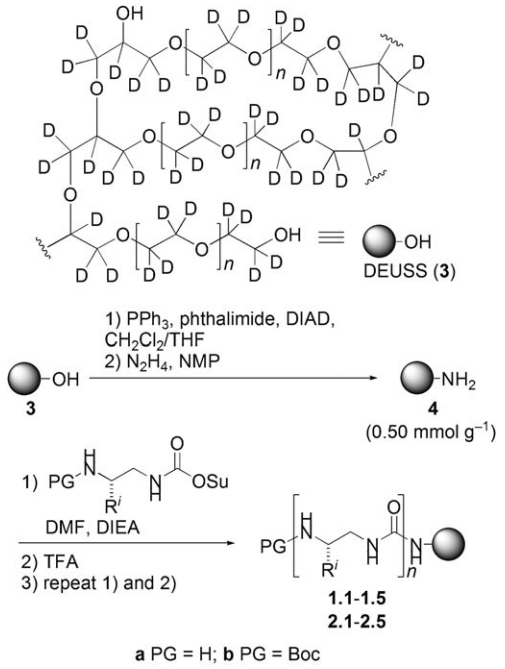

Scheme 1. Preparation of the two series of DEUSS-immobilized *N*,*N*′-linked oligoureas **1** and **2**.

ea **1.4** proved to be very difficult due to lower quality spectra, poor signal dispersion, and/or missing resonances. The problems of missing resonances and poor spectrum resolution can be ascribed to a lack of mobility of the oligomeric chain, to aggregation, and/or to the presence of different conformations in equilibrium. Such difficulties have been encountered previously during HRMAS analyses of resin-bound peptides on various types of solid support.[9a,11,14] In contrast, nicely resolved spectra were obtained for DEUSS-bound hexaurea **1.5a** swollen in [D_3]MeCN. DIPSI2 and ^{1}H-^{13}C HSQC measurements allowed the assignment of proton resonances for all residues. The fingerprint NH/$^{\beta}$CH and N′H/$^{\alpha}$CH region in the DIPSI2 experiment is shown in Figure 2b. Almost all crosspeaks were properly resolved. The ^{1}H-^{13}C HSQC experiment was extremely useful to confirm chemical shifts of diastereotopic $^{\alpha}$CH protons. The sequence-specific assignment of all resonances was achieved by NOESY experiments (mixing time $\tau_m = 300$ ms) and was deduced from the strong N′H(i+1)–NH(i) NOE connectivities within urea bonds. HRMAS analysis of resin-bound oligoureas **2** was less problematic and spin systems of all residues were observed in compounds **2.1**–**2.5**. Again, resolution and signal dispersion of ^{1}H-^{13}C HSQC spectra increased with the length of the oligomers to reach a maximum for hexaureas **2.5a** and **2.5b** (see Figure 2c). It is worth noting that all N′H(i+1)–NH(i) NOE correlations were observed in **2.5b** (see Supporting Information).

We previously reported that the chemical shift difference ($\Delta\delta$) between diastereotopic $^{\alpha}$CH protons is a useful descriptor of the conformational homogeneity of helical *N*,*N*′-linked oligoureas. In the case of a 2.5-helical heptaurea, $\Delta\delta$ values as high as 1.5 and 1.3 ppm have been measured for

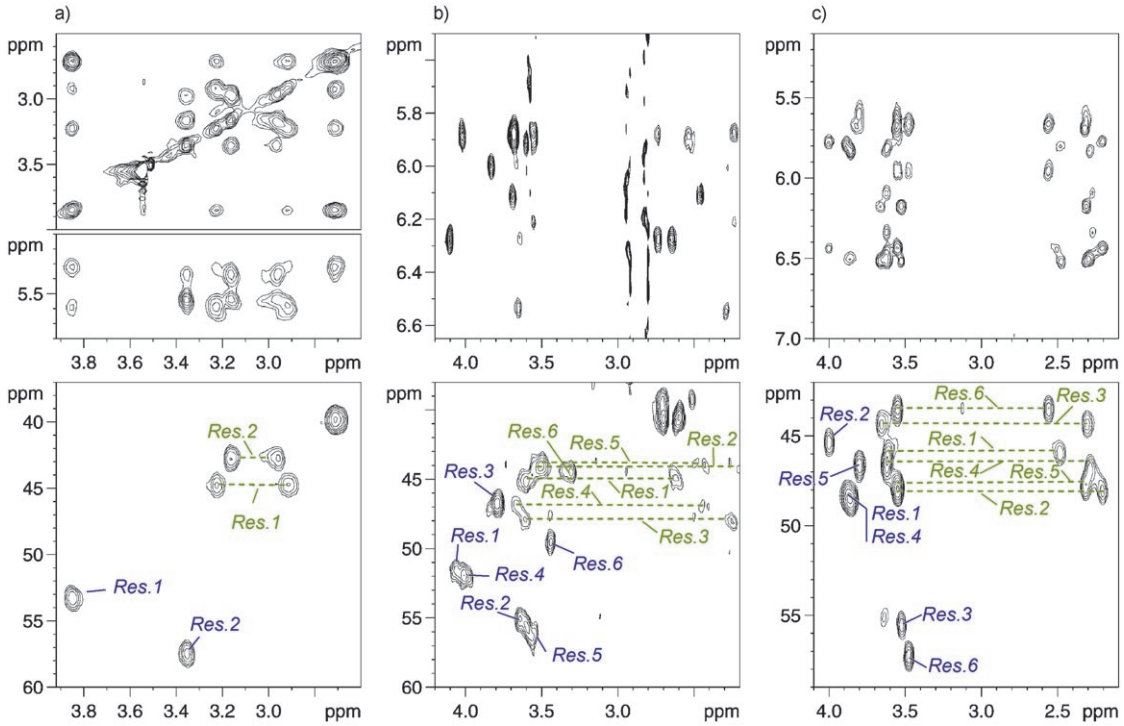

Figure 2. Parts of the 500 MHz DIPSI2 (top) and ^{1}H-^{13}C HSQC plots (bottom) of DEUSS-bound oligoureas: a) **1.1b**, b) **1.5a**, and c) **2.5b** recorded in [D_3]MeCN at 300 K. H–$^{\beta}$C and H–$^{\alpha}$C cross-peaks in the ^{1}H-^{13}C HSQC plots are indicated in blue and green, respectively.

central residues in [D_5]pyridine (300 K) and [D_3]methanol (300 K), respectively.[5a–c] This parameter can also be used to compare oligomers differing in both length and sequence. In this study, it was possible to extract $\Delta\delta$ values for oligoureas **1.5a**, **1.5b**, **2.1a**–**2.5a**, and **2.5b** from their DIPSI2 and ^{1}H-^{13}C HSQC spectra. Examination of $\Delta\delta$ values of residues 1 and 2 in oligomers **2.1a**–**2.5a** revealed a dramatic change (e.g. from 0.34 to 1.25 ppm for residue 2) as the length of the chain increased from four to five residues (Figure 3).

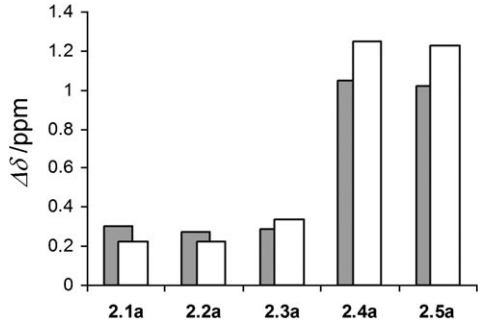

Figure 3. Variation of the chemical shift differences ($\Delta\delta$) between geminal $^{\alpha}$CH protons of residues 1 (grey bars) and 2 (white bars) as a function of chain length. $\Delta\delta$ values were extracted from DIPSI2 and ^{1}H-^{13}C HSQC spectra of oligoureas **2.1a**–**2.5a** recorded in [D_3]MeCN at 300 K.

This increase in $\Delta\delta$ with a single-residue chain-length increment is much sharper than previously observed in solution for another sequence[5c] and suggests, that in this case, a five residue length is an absolute requirement for helix nucleation.

The effect of capping the free amino group on the chemical shift differences ($\Delta\delta$) between geminal $^{\alpha}$CH protons has been examined in both sequences. The $\Delta\delta$ values were measured for residues 1–6 in oligoureas **1.5a**, **2.5a** (Figure 4a), **1.5b** and **2.5b** (Figure 4b).

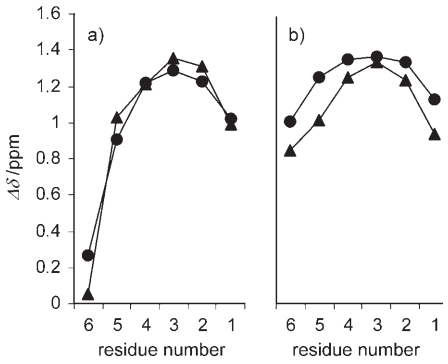

Figure 4. Effects of sequence and capping of the free amino group on the chemical shift differences ($\Delta\delta$) between geminal $^{\alpha}$CH protons in oligourea hexamers: a) $\Delta\delta$ values are reported for residues 1–6 in hexamers **1.5a** (triangles) and **2.5a** (circles); b) $\Delta\delta$ values are reported for residues 1–6 in hexamers **1.5b** (triangles) and **2.5b** (circles). $\Delta\delta$ values were extracted from DIPSI2 and ^{1}H-^{13}C HSQC experiments recorded in CD_3CN at 300 K.

As shown in Figure 4a, **1.5a** and **2.5a** display an almost identical $\Delta\delta$ signature, typical for helix-forming oligoureas, with $\Delta\delta$ values for central residues 2–4 above 1.2 ppm. In agreement with previous studies in solution, the first and penultimate residues exhibit somewhat lower values ($\approx$1 ppm), whereas the amino terminal residue is characterized by almost no diastereotopy of its methylene protons. When examining N-capped hexamers, the situation is clearly different between the two sequences, oligourea **2.5** being more sensitive to capping than **1.5**. This is particularly striking for the penultimate residue, which exhibits a 0.33 ppm shift towards higher $\Delta\delta$ values in the case of **2.5b**, while in the **1.5** series, the same residue is not sensitive to capping. Finally, all residues in **2.5b** exhibit slightly higher $\Delta\delta$ values than in **1.5b** thus suggesting that **2.5b** might adopt a more stable 2.5-helical conformation than **1.5b**. Overall, these results suggest that, if applied to a larger set of oligourea sequences, this approach can be used to delineate the relationship between side chain structure and 2.5-helix stability in oligourea foldamers.

Influence of the solvent: Among the many parameters that may affect the folding propensity and the conformational stability of oligoureas, the solvent is one of the most important. It also one of the easiest to vary during HRMAS NMR studies of grafted oligoureas, by simply filtering, rinsing, and drying the resin prior to change the solvent. Furthermore, it is possible to include solvents in which oligoureas are poorly soluble as long as high swelling of the resin is maintained. Previous structural analysis of a oligourea heptamer in solution suggested that the 2.5-helix is more stable in pyridine than in methanol.[5c] To further document the influence of the solvent on the folding propensity of oligoureas, we have now undertaken HRMAS NMR analysis of DEUSS-supported hexaurea **2.5a** in aprotic solvents ranging from low (pyridine) to high (DMSO) polarity as well as in protic solvents (MeOH, H_2O). DEUSS[16] like POEPOP[17] and other PEG-cross-linked resins (e.g., PEGA,[21] SPOCC,[22] ChemMatrix[23]) and PEG-grafted resins (e.g. PEG-PS,[24] TentaGel,[25] PVAg-PEG[26]) display optimal swelling capacity in a variety of nonpolar and polar solvents including water, and are thus particularly well suited for studying solvent effects by HRMAS NMR spectroscopy.[27]

In pyridine, acetonitrile, methanol, and DMSO, signals were well dispersed and complete spin-system assignment was readily achieved from DISPI2 and ^{1}H-^{13}C HSQC experiments. Both ^{1}H and ^{13}C chemical shifts of **2.5a** swollen in [D_5]pyridine are collected in Tables S1 and S2 of Supporting Information. Parts of the ^{1}H-^{13}C HSQC plots with assigned H-$^{\alpha}$C correlations in all four solvents are shown Figure 5. However, spin system assignment of **2.5a** swollen in water was hampered by the poor dispersion of the signals (see the Supporting Information).

We were able to measure $\Delta\delta$ values between geminal $^{\alpha}$CH protons with precision for all six residues in all solvents except water. A $\Delta\delta$ signature typical of the helical fold was observed in pyridine, acetonitrile, methanol, and even

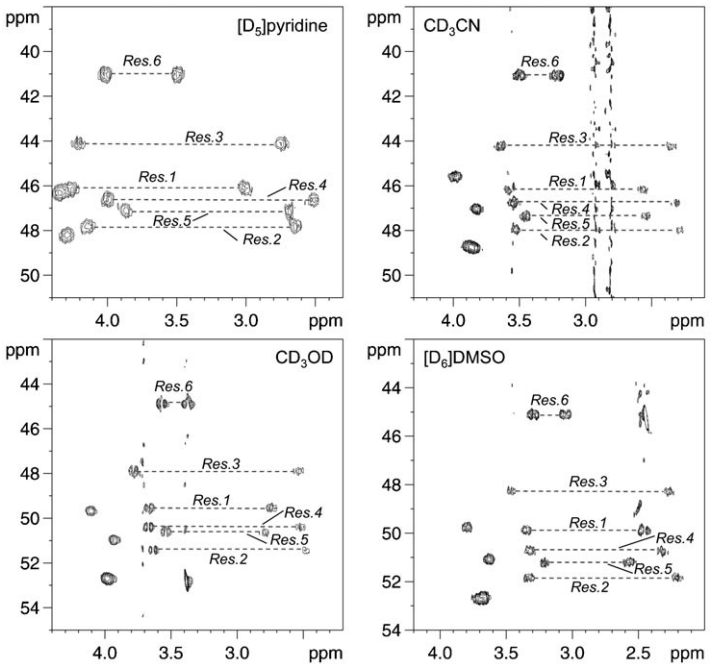

Figure 5. Parts of the 500 MHz ^{1}H-^{13}C HSQC plot showing H–$^{\alpha}C$ correlation for all six residues of **2.5a** swollen in pyridine, acetonitrile, methanol, or DMSO.

DMSO, with the highest $\Delta\delta$ values being observed for residues 2–4 ($\Delta\delta > 1$ ppm) (Figure 6).

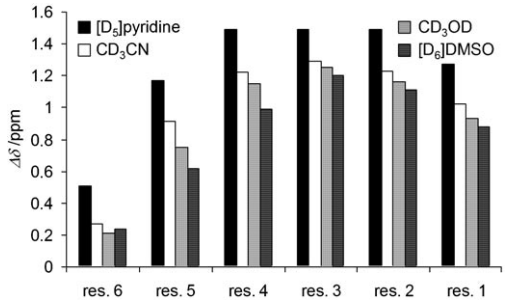

Figure 6. Solvant effect on the chemical shift differences between geminal $^{\alpha}CH$ protons of residues 1–6 in oligourea **2.5a** at 300 K.

In water, $\Delta\delta$ values could not be determined with confidence due to the lack of spectrum resolution (limited signal dispersion and line broadening). Examination of the ^{1}H-^{13}C HSQC plot revealed that $\Delta\delta$ values do not exceed 0.4–0.6 ppm (see the Supporting Information). Overall the HRMAS NMR spectrum of **2.5a** in D_2O is likely to reflect equilibrium between partially folded/unfolded conformations, and demonstrate the lower propensity of uncapped hexaurea **2.5a** for helical folding in aqueous solution.

In pyridine, acetonitrile, methanol, and DMSO, the $\Delta\delta$ values obtained for the amino terminal residue 6 (between 0.21–0.51 ppm) was much lower than the values for other residues in the sequence. This is compatible with helix fraying at the amino terminal end. Comparison of $\Delta\delta$ values all along the main chain was very instructive to rank the solvents according to their propensity to stabilize 2.5-helical folding of hexaurea **2.5a**. The following order was inferred from $\Delta\delta$ values reported in Figure 6: pyridine $\gg$ acetonitrile > methanol > DMSO $\gg$ water. In good agreement with the results previously obtained in solution, the $\Delta\delta$ values observed here for **2.5a** confirm that pyridine is the solvent that stabilizes helical folding the most. It is worth noting that $\Delta\delta$ values obtained by HRMAS NMR spectroscopy for **2.5a** swollen in CD_3OD compare very well with those previously extracted by NMR spectroscopy in CD_3OH for another hexaurea sequence consisting of Val, Ala, and Tyr side chains (i.e. compound **3** in reference [5c]).[28]

To gain more information about the three-dimensional structure of DEUSS supported hexaurea **2.5a** swollen in pyridine, NOESY experiments were acquired at 300 K with a mixing time of 300 ms (Figure 7). The sequence-specific assignment was deduced from the strong $N'H(i+1)$–$NH(i)$ NOE connectivities (see Figure 7c).

Inspection of medium-range interesidue NOEs was particularly informative. The presence of all possible ($i=1$ to 4) $NH(i)/^{\beta}CH(i+2)$, and $N'H(i)/^{\beta}CH(i+2)$ NOE connectivities as well as of two cross peaks between $NH(i)$ and the downfield $^{\alpha}CH(i+2)$ was highly consistent with **2.5a** adopting a 2.5 helical fold in pyridine (Figure 7). This characteristic NOE pattern is a common feature of all oligoureas found to adopt a 2.5-helical structure.[5a–c]

Conclusion

By this study, we have shown that HRMAS NMR spectroscopy is a practical technique for screening and studying the preferential conformations of biotic *N*,*N*′-linked oligoureas. One of the major advantages of this approach is that only minute amounts of material, that is, typically 1–2.5 μmol of immobilized oligoureas, are required. Our motivation to use DEUSS, a perdeuterated PEG-crosslinked resin previously developed in our laboratories, for oligourea attachment stemmed from: 1) its high swelling properties in a wide range of polar and nonpolar solvents, 2) the good resolution of HRMAS NMR spectra of compounds bound to DEUSS compared to other solid-supports, and 3) the remarkable reduced intensity of the oxyethylene proton signal compared to POEPOP, its nondeuterated version. Detailed HRMAS NMR analysis in CD_3CN of a series of DEUSS-bound oligoureas differing in either chain length, sequence, or capping mode revealed a number of interesting features. Although the signal resolution of DEUSS-bound oligourea spectra remains lower than that observed for oligoureas by liquid-state NMR spectroscopy in corresponding solvents, (i.e. coupling constants cannot be extracted from HRMAS NMR spectra) the signals were sufficiently dispersed for complete spin-system identification and sequence assignment. In addition, chemical shifts of diasterotopic $^{\alpha}CH$ protons were readily extracted from DISPSI2 and ^{1}H-^{13}C HSQC experiments and provided reliable qualitative infor-

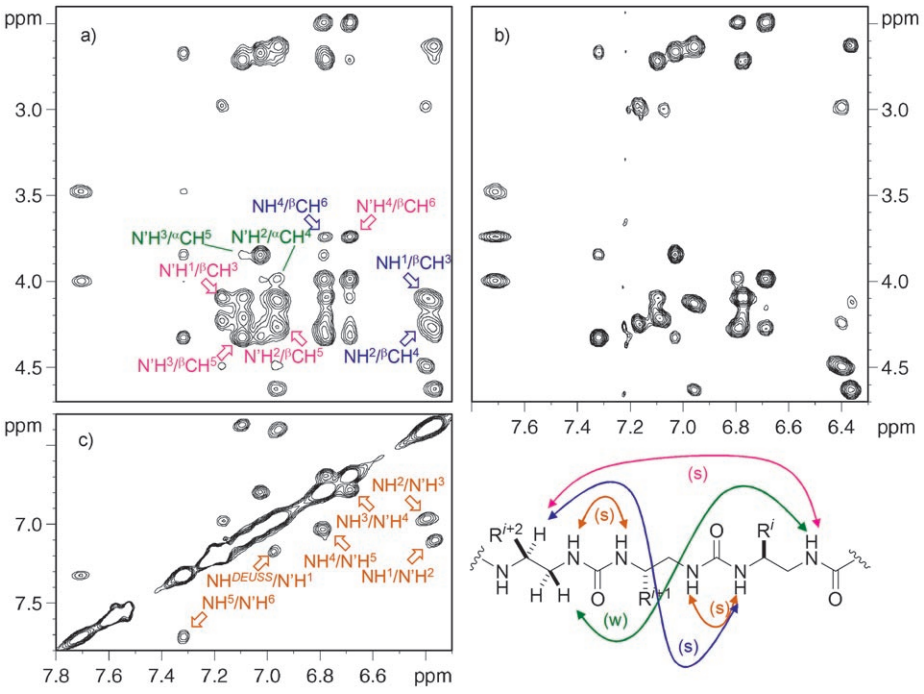

Figure 7. Representative sets of NOE connectivities observed for **2.5a** in [D_5]pyridine at 300 K. a) NOESY plot ($\tau_m = 300$ ms) showing all inter-residue NH(i)/$^{\beta}$CH(i+2) (blue) and N′H(i)/$^{\beta}$CH(i+2) (pink) ($i = 1$, 2, 3, and 4) as well as some N′H(i)/$^{\alpha}$CH$_{Si}$(i+2) crosspeaks (green). These $i/i+2$ NOE connectivities are consistent with **2.5a** adopting the canonical 2.5-helical structure of oligoureas. b) The corresponding part of the TOCSY plot ($\tau_m = 60$ ms) is shown for comparison. c) Part of the NH/NH region of the NOESY plot ($\tau_m = 300$ ms) of **2.5a** recorded at 300 K. All interresidue NH(i)/N′H(i+1) NOEs (orange) are observed and were used for sequence assignment Residues are numbered consecutively from 1 to 6 as displayed in Figure 1.

mation about folding propensity of oligoureas. In the compound **2** series, a single-residue chain-length increment from tetramer to pentamer was found sufficient to promote 2.5-helix nucleation, thus, suggesting that five residues represent the minimum chain length to stabilize the 2.5-helical fold. Whereas in the uncapped series sequence variation had negligible influence on helix propensity of hexaureas, a significant sequence effect was observed in the *N*-Boc-protected series. Hexaurea **2.5b** with aliphatic side chains displayed for example systematically higher $\Delta\delta$ values than **1.5b**. This approach based on $\Delta\delta$ value determination is very promising to screen larger arrays of resin-bound oligoureas and to further delineate the requirements for helix formation (e.g., relationship between 2.5-helix formation and the structure of side chains and primary sequence). The influence of the surrounding environment, that is, the solvent, on 2.5-helix population was also investigated. In the case of hexaurea **2.5a**, although helix formation was maximized in a low polar environment (pyridine), significant helix population was retained in both protic and polar aprotic media (MeCN > MeOH > DMSO). The low resolution of the spectrum in D_2O precluded detailed insight of the structure of **2.5a** in water. According to estimated $\Delta\delta$ values, uncapped hexaurea **2.5a** is likely to be only partially folded in aqueous environment, thus suggesting that capping and/or longer chain length are required to increase helix propensity. This is confirmed by early CD investigations of antibacterial oligoureas. Significant helix population was retained in hepes buffer saline (HBS) pH 7.4 for longer *N*-capped oligomers (e.g., nonamers).[7] Such amphiphilic cationic oligoureas retained high helix propensity (similar to what is found in MeOH) in the presence of negatively charged PC:PG (70:30; PC = phosphatidylcholine, PG = phosphatidylglycerol) small unilamellar vesicles (SUV) and are fully bactericidal. Overall, this suggests that despite modest helicity in water, the helical folding propensity can be increased significantly in biomolecular recognition events. Although helicity in water is intrinsically weaker than in other polar and apolar solvents, several strategies inspired by work on α- and β-peptides,[1–4,29] to design oligoureas with a high level of helicity in aqueous media are worth being evaluated in the future. These include: 1) the formation of salt bridges between overlapping side chains, 2) the maximization of electrostatic interactions with the helix macrodipole, and 3) the incorporation of residues with increased backbone preorganization.

As exemplified by the analysis of hexaurea **2.5a** swollen in pyridine, HRMAS NMR NOESY experiments allowed extraction of most medium range (i)–(i+2) NOE correlations associated with the 2.5-helical structure. This result demonstrates that HRMAS NMR analysis of oligoureas is not limited to qualitative structural description based on the determination of $\Delta\delta$ values but is a powerful technique to gain detailed structural information on oligoureas by integration of distance restraints.

Experimental Section

Synthesis of oligoureas immobilized on DEUSS: Assembly of oligoureas **1** and **2** was carried out on a 2.5 μmol scale starting from DEUSS **4**[16] and using succinimidyl-2-[(*tert*-butoxycarbonyl)amino]-2-substituted ethyl carbamates.[18] For each coupling step, a solution of the appropriate carbamate (5 equiv) in DMF (300 μL) and diisopropylethylamine (DIEA; 10 equiv) were added subsequently to the resin. The suspension was shaken for 2 h at room temperature and a double coupling was performed systematically. At the end of the reaction, the resin was washed with DMF (6 × 300 μL). The Boc group was removed by treatment with TFA (300 μL, 2 × 5 min) and the resin was washed with CH_2Cl_2, *i*PrOH,

and DMF. The final ureas on solid support were washed with CH_2Cl_2 and diethyl ether, and dried under vacuum at 50 °C for 12 h.

HRMAS NMR spectroscopy: The identification of amino acid spin systems and sequential assignment were made by using a combination of HRMAS TOCSY,[30] NOESY,[31] and HSQC[32] experiments. HRMAS 1D and 2D NMR spectra were obtained on a Bruker Avance 700 MHz spectrometer equipped with for 4 mm $^1H/^{13}C/^{15}N/^2H$ HRMAS gradient probe or on a Bruker DSX 500 MHz spectrometer equipped with for 4 mm HXMAS4 ($^1H/X$, X tuned to ^2H) or with for HXY ($^1H/X/Y$, X tuned to ^{13}C and Y tuned to ^2H) probe. The samples (3–5 mg) were packed into a 4 mm HRMAS rotor and solvents were added to the resin directly inside the rotor. Samples were spun at 6–7 kHz. The spectra were acquired at 300 K and referenced to the peak of the solvent. All 2D homonuclear spectra were recorded in pure phase mode by using the States-TPPI method. Homonuclear spectra were recorded with 2048 data points in t_2 and 256 or 512 increments in t_1. Typically 8 or 32 scans per increment were accumulated. A spectral width of 5482.46 Hz was used for the proton. TOCSY data were recorded with a DIPSI2[33] sequence of 60 ms. Through-space dipolar connectivities were obtained from NOESY spectra by using mixing times from 300 ms. All 2D heteronuclear spectra were recorded in the pure phase mode by using the States-TPPI or Echo-Antiecho TPPI method. ^1H-^{13}C HSQC spectra were recorded with 1024 or 2048 data points in t2 and 256 or 512 increments in t_1. The number of scans accumulated for ^1H-^{13}C HSQC were 32 or 44. Sweep widths for ^1H and ^{13}C dimensions were 5482.46 Hz and 12722 Hz, respectively. The samples were swollen in [D_5]pyridine, [D_6]DMSO, CD_3CN, CD_3OD and D_2O.

Acknowledgements

This research was supported in part by Centre National de la Recherche Scientifique (CNRS), Agence Nationale pour la Recherche (grant no. NT05-4-42848), Région Alsace, and ImmuPharma France. Pre-doctoral grants from Region Alsace and ImmuPharma France (A.V.) as well as from Bruker and CNRS (N.L.) are gratefully acknowledged.

[1] *Foldamers: Structure, Properties and Applications*, (Eds.: S. Hecht, I. Huc), Wiley-VCH, Weinheim, **2007**.

[2] G. Guichard in *Pseudopeptides in Drug Development*, (Ed.: P. E. Nielsen), Wiley-VCH, Weinheim, **2004**, pp. 33–120.

[3] D. Seebach, A. K. Beck, D. J. Bierbaum, *Chem. Biodiversity* **2004**, *1*, 1111–1239.

[4] D. J. Hill, M. J. Mio, R. B. Prince, T. S. Hughes, J. S. Moore, *Chem. Rev.* **2001**, *101*, 3893–4011.

[5] a) V. Semetey, D. Rognan, C. Hemmerlin, R. Graff, J.-P. Briand, M. Marraud, G. Guichard, *Angew. Chem.* **2002**, *114*, 1973–1975; *Angew. Chem. Int. Ed.* **2002**, *41*, 1893–1895; b) C. Hemmerlin, M. Marraud, D. Rognan, R. Graff, V. Semetey, J.-P. Briand, G. Guichard, *Helv. Chim. Acta* **2002**, *85*, 3692–3711; c) A. Violette, M. C. Averlant-Petit, V. Semetey, C. Hemmerlin, R. Casimir, R. Graff, M. Marraud, J.-P. Briand, D. Rognan, G. Guichard, *J. Am. Chem. Soc.* **2005**, *127*, 2156–2164; d) M. T. Oakley, G. Guichard, J. D. Hirst, *J. Phys. Chem. B* **2007**, 111, 3274–3279.

[6] a) V. Semetey, C. Hemmerlin, C. Didierjean, A. P. Schaffner, A. G. Giner, A. Aubry, J.-P. Briand, M. Marraud, G. Guichard, *Org. Lett.* **2001**, *3*, 3843–3846; b) L. Fischer, V. Semetey, J. M. Lozano, A. P. Schaffner, J.-P. Briand, C. Didierjean, G. Guichard, *Eur. J. Org. Chem.* **2007**, 2511–2525.

[7] a) L. Xing, U. Ziener, C. Todd C. , L. A. Cuccia, *Chem. Commun.* **2005**, 5751–5753; b) A. Zhang, Y. Han, K. Yamato, X. C. Zeng, B. Gong, *Org. Lett.* **2006**, *8*, 803–806; c) R. W. Sinkeldam, M. H. C. J. van Houtem, K. Pieterse, J. A. J. M. Vekemans, E. W. Meijer, *Chem. Eur. J.* **2006**, *12*, 6129–6137; d) J. M. Rodriguez, A. D. Hamilton, *Angew. Chem.* **2007**, *119*, 8768–8771; *Angew. Chem. Int. Ed.* **2007**, *46*, 8614–8617

[8] A. Violette, S. Fournel, K. Lamour, O. Chaloin, B. Frisch, J.-P. Briand, H. Monteil, G. Guichard, *Chem. Biol.* **2006**, *13*, 531–538.

[9] a) C. Dhalluin, C. Boutillon, A. Tartar, G. Lippens, *J. Am. Chem. Soc.* **1997**, *119*, 10494–10500; b) R. Warras, J. M. Wieruszeski, C. Boutillon, G. Lippens, *J. Am. Chem. Soc.* **2000**, *122*, 1789–1795.

[10] R. Jelinek, A. P. Valente, K. G. Valentine, S. J. Opella, *J. Magn. Reson.* **1997**, *125*, 185–187.

[11] K. Elbayed, M. Bourdonneau, J. Furrer, T. Richert, J. Raya, J. Hirshinger, M. Piotto, *J. Magn. Reson.* **1999**, *136*, 127–129.

[12] C. H. Gotfresden, M. Grtli, M. Willert, M. Meldal, J. Ø. Duus, *J. Chem. Soc. Perkin Trans. 1* **2000**, 1167–1171.

[13] A. Bianco, J. Furrer, D. Limal, G. Guichard, K. Elbayed, J. Raya, M. Piotto, J.-P. Briand, *J. Comb. Chem.* **2000**, *2*, 681–690.

[14] J. Furrer, M. Piotto, M. Bourdonneau, D. Limal, G. Guichard, K. Elbayed, J. Raya, J.-P. Briand, A. Bianco, *J. Am. Chem. Soc.* **2001**, *123*, 4130–4138.

[15] a) N. Lancelot, K. Elbayed, J. Raya, M. Piotto, J.-P. Briand, F. Formaggio, C. Toniolo, A. Bianco, *Chem. Eur. J.* **2003**, *9*, 1317–1323; b) M. Rainaldi, N. Lancelot, K. Elbayed, J. Raya, M. Piotto, J.-P. Briand, B. Kaptein, Q. B. Broxterman, A. Berkessel, F. Formaggio, C. Toniolo, A. Bianco, *Org. Biomol. Chem.* **2003**, *1*, 1835–1837.

[16] A. Poschalko, N. Lancelot, J. Marin, V. Larras, D. Limal, K. Elbayed, J. Raya, M. Piotto, J. P. Briand, G. Guichard, A. Bianco, *Chem. Eur. J.* **2004**, *10*, 4532–4537.

[17] M. Renil, M. Meldal, *Tetrahedron Lett.* **1996**, *37*, 6185–6188.

[18] G. Guichard, V. Semetey, C. Didierjean, A. Aubry, J.-P. Briand, M. Rodriguez, *J. Org. Chem.* **1999**, *64*, 8702–8705.

[19] G. Guichard, V. Semetey, M. Rodriguez, J.-P. Briand, *Tetrahedron Lett.* **2000**, *41*, 1553–1557.

[20] Whereas Fmoc/*t*Bu chemistry on solid support was found previously to be convenient for oligourea synthesis, it showed some limitations in the course of the synthesis of a number of oligoureas, which were recovered in low yields after HPLC purifications. The main problems observed with *N*-Fmoc protected building blocks include poor coupling and/or poor Fmoc-deprotection yields associated with monomer decomposition and some double coupling reactions for oligomers >5-mers. The presence of many impurities in the crude product is not compatible with the quality required for direct HRMAS NMR analysis. Re-investigation of the more robust *N*-Boc protected monomers demonstrated the superiority of Boc chemistry for solid phase preparation of oligoureas in high yield and purity.

[21] M. Meldal, *Tetrahedron Lett.* **1992**, *33*, 3077–3080.

[22] J. Rademann, M. Grøtli, M. Meldal, K. Bock, *J. Am. Chem. Soc.* **1999**, *121*, 5459–5466.

[23] F. Garcia-Martin, M. Quintanar-Audelo, Y. Garcia-Ramos, L. J. Cruz, C. Gravel, R. Furic, S. Cote, J. Tulla-Puche, F. Albericio, *J. Comb. Chem.* **2006**, *8*, 213–220.

[24] S. A. Kates, B. F. McGuinness, C. Blackburn, G. W. Griffin, N. A. Sole, G. Barany, F. Albericio, *Biopolymers* **1998**, *47*, 365–380.

[25] W. Rapp, in *Combinatorial Peptide and Nonpeptide Libraries: A Handbook* (Ed.: G. Jung), VCH, Weinheim, Germany, **1996**, pp. 425–464.

[26] J. Luo, C. Pardin, X. X. Zhu, W. D. Lubell, *J. Comb. Chem.* **2007**, *9*, 582–591.

[27] M. Grotli, C. H. Gotfredsen, J. Rademann, J. Buchardt, A. J. Clark, J. O. Duus, M. Meldal, *J. Comb. Chem.* **2000**, *2*, 108–119.

[28] It is important to note that oligourea concentrations differ significantly between solution NMR and HRMAS NMR experiments. The concentration of DEUSS-linked oligourea **2.5a** can be estimated as follows. The substitution of the starting resin **4** is 0.5 mmol g^{-1}. Assuming a quantitative synthesis, the final loading of **2.5a** is 0.36 mmol g^{-1}. A batch of 4 mg of resin used in HRMAS experiments thus represents 1.44 μmol of oligomer. The maximum volume of the HRMAS rotor being 50 μL, this makes the final concentration of **2.5a** in the rotor of about 30 mM, which is approximately 10 times more concentrated that hexaurea **3** studied in reference [5c] (3 mM). The very limited variation of ($\Delta\delta$) values exctracted from NMR spectra of **2.5a** and **3** (see Supporting Information) suggests that the overall conformation does not change significantly when

the concentration rises from 3 mM (in solution) to 30 mM (on the support).
[29] M. J. I. Andrews, A. B. Tabor, *Tetrahedron* **1999**, *55*, 11711–11743.
[30] L. Braunschweiler, R. R. Ernst, *J. Magn. Reson.* **1983**, *53*, 521–528.
[31] J. Jeneer, B. H. Meier, P. Bachmann, R. R. Ernst, *J. Chem. Phys.* **1979**, *71*, 4546–4553.
[32] G. Bodenhausen, D. J. Ruben, *Chem. Phys. Lett.* **1980**, *69*, 185–189.
[33] A. J. Shaka, C. J. Lee, A. Pines, *J. Magn. Reson.* **1988**, *77*, 274–293.

Received: December 5, 2007
Published online: March 28, 2008

